Fusion Engineering and Design 204 (2024) 114486

Contents lists available at ScienceDirect

Fusion Engineering and Design

journal homepage: www.elsevier.com/locate/fusengdes

Operation of a 250μm-thick SiC detector with DT neutrons at high temperatures

Matteo Hakeem Kushoro [a,b,*], Maurizio Angelone [c], Daniele Bozzi [a], Stephanie Cancelli [a,b], Andrea Dal Molin [b], Erik Gallo [d], Giuseppe Gorini [a], Francesco La Via [e], Miriam Parisi [d], Enrico Perelli Cippo [b], Oscar Putignano [b], Marco Tardocchi [b], Marica Rebai [b]

[a] Department of Physics "G. Occhialini", University of Milano-Bicocca, Piazza dell'Ateneo Nuovo 1, 20126, Milano, Italy
[b] Institute for Plasma Science and Technology (CNR), Via Roberto Cozzi 53, 20125, Milano, Italy
[c] ENEA, Fusion and Technology for Nuclear Safety and Security Department, Via E. Fermi 45 00044, Frascati, Italy
[d] Eni S.p.A MFI – Magnetic Fusion Initiative, San Donato Milanese, Italy
[e] Institute for Microelectronics and Microsystems, CNR 95121 Catania, Italy

ARTICLE INFO

Keywords:
Silicon Carbide Detector
Neutron Detection
Fusion Plasma Diagnostics
Breeding Blanket
High Temperature
Frascati Neutron Generator

ABSTRACT

The Silicon Carbide detector (SiC) is an object of research as an alternative to diamond detectors for fast neutron detection and spectrometry where harsh environments are an issue, like in Tokamaks. Since future breeding blankets mock-ups will feature temperatures up to 550 °C, diamond detectors were characterized in the past, finding limitations in their functionality at high temperatures. This paper expands on the previous work by proving the detection of fast neutrons with good detection parameters of a 250 μm-thick 4 H-SiC detector prototype at temperatures up to 250 °C, highlighting the detector's excellent resilience to temperature. The experiment is conducted with instrumentation similar to the one used in the past with diamond detectors, using as source of irradiation the Frascati Neutron Generator (FNG) in ENEA, which is accelerator driven neutron source based on deuterium-tritium (DT) fusion reaction.

1. Introduction

The construction of high-power fusion plasma machines, like ITER, is driving the interest toward the development and refining of tokamak technologies. Among those, one critical aspect is the supply of tritium, the production of which is planned to be done in the Breeding Blanket (BB) – a physical region close to the plasma where neutrons interact with Li (after being slowed and multiplied) producing tritium through the ^{6}Li (n,α)T and ^{7}Li(n,n+α)T reactions. To date, no volumetric neutron sources with fluences comparable to the ones in a tokamak exist where to test the BB designs [1]. The first of this type of sources will probably be ITER, which will feature a series of Test Blanket Modules (TBM) to experiment four possible designs of tritium production and fuel cicle [2]. ITER's data will then be used as a basis for the DEMO design [1]. On the other hand, ARC (the successor of SPARC) is prospected to feature a tritium cycle based on liquid metal [3] which is still in the conceptual design phase. In any case, to date the knowledge about the practical application of tritium production is partial and limited to numerical simulations. This makes the ground fertile for the development of diagnostics to be installed in future BB experiments, the data of which could be instrumental in validating the simulations.

In order to be used inside the BB fast neutron detectors are required to feature small dimensions, intense flux measurement capabilities and high radiation hardness. It is also required for them to be able to withstand high temperatures, since the temperature range expected inside ITER's TBM is between 300 °C and 550 °C [4]. Both Single Crystal Diamond detectors (SCDs) [5,6,7] and Silicon Carbide detectors (SiCs) [8,9,10] were characterized in the past, prospecting them as good candidates for neutron detection in tokamak's harsh environments. In fact, diamond detectors are already used at JET [11] and are part of the design of future tokamaks neutron cameras [12]. The response of diamond under high temperature (HT) was also studied [5,13,14], finding a strong dependence on the type of electrode deposition, material and the size of the active volume. Various diamond featured a response declining in quality after 200 °C, making them not ideal candidates for BB neutron detection. On the other hand, functionality of SiC under HT

* Correspondence author.
E-mail address: matteo.kushoro@unimib.it (M.H. Kushoro).

https://doi.org/10.1016/j.fusengdes.2024.114486
Received 10 October 2023; Received in revised form 5 April 2024; Accepted 30 April 2024
Available online 8 May 2024

was proven on a few occasions (e.g.: [15,16]), achieving very promising results. The scope of this paper is then to make the first step towards the characterization of the HT behaviour of the SiC detectors already tested in the past.

2. Instrumentation and Setup

2.1. Detectors

The detector under test is made on a 4H-SiC substrate with a new epitaxy process developed by CNR-IMM in collaboration with ASM in Catania, similarly to the detector tested in the past [9,17–20]. The crystal is a 250 μm thick and has a surface $5 \times 5\ mm^2$. The structure of the device differs from the one of the detectors tested in [19] and [20] since it is arranged in a p-n junction structure as opposed as a Schottky contact. The edge structure was also manufactured with a higher quality, in order to achieve a higher voltage breakdown than the one experimented in [19] and [20]. For the structure and manufacturing of the detector device refer to [21,22], while for the specifics of the epitaxy used in this work refer to [23].

Electrodes connecting the crystal to the signal cable are much different than the ones used in the past. Instead of being welded on a conducting surface of a printed circuit board, the detector was contacted through pressure, being closed between a solid cable (acting as the line transmitting the HV and the signal) and a stainless-steel support, whose purpose was to keep the detector in place as well as connecting the p-region to the ground. The reason for choosing a pressure contact was to avoid components incapable to withstand high temperatures without melting or altering electric properties. A picture of the detectors can be seen in Fig. 1, while the support and the contacting can be seen in Fig. 2. All the device was then enveloped in conducting tape (connected to the same ground reference of the cable) in order to reduce EM noise.

2.2. Cables and Electronics

The signals collected by the detector were processed by a Cividec SiC preamplifier, which was custom developed on the Cividec CX-L amplifier [24] in order to work on reverse polarities. The signal was then fed to an analog-to-digital convertor 500 MHz CAEN 5730 [25]. Both elements are the same used in the past for 250 μm thick detectors ([19]). The transmission of the signal (and the supply of the HV to the detector) was performed through a mineral insulated cable manufactured by Thermocoax which features low thermal noise and is certified to

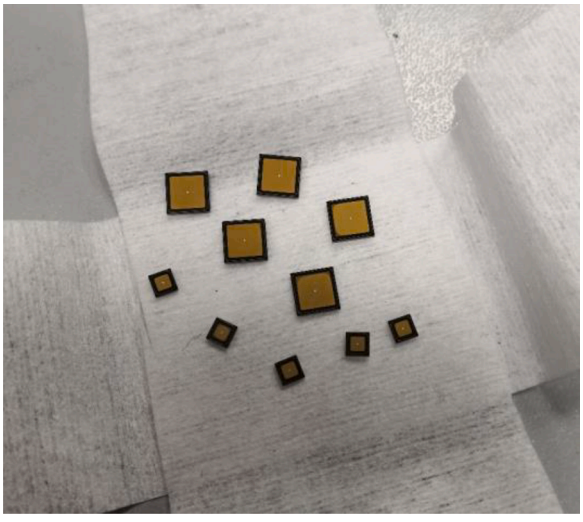

Fig. 1. SiC250 p-n detectors. The one used in this work is one of the widest on top, measuring $5 \times 5\ mm^2$ in area.

Fig. 2. SiC250 detector with the pressure contacts. The T-shaped steel support is on the left and can move parallel to the mineral cable (on the right) in order to push the signal pin (in the centre) against the detector, keeping it in position.

temperatures up to 1200 °C. The cable was the same used for the diamond detectors by Angelone in [13]: the choice was done in order to trace a comparison between the diamond and the SiC with as few differing elements in the setup as possible.

2.3. Heating System

The high temperatures were achieved through an oven constituted by a resistive spiral winded around a metallic cylinder. The inside of the cylinder is hollow, allowing for the detector and the cable to be inserted from one of the two ends. The cylinder is covered in a thermal insulating foam in order to increase its thermal capacity and allow to soften the temperature gradients, both temporally and spatially. The temperature control was achieved by controlling the amperage of the current flowing through the resistance. The temperature was read through a small (mm-thin) thermistor, with a nominal precision of 0.1 °C. The feedback cycle was performed by hand, altering the current to increase, decrease or keep stable the temperature. The heating system is depicted in Fig. 3.

2.4. Neutron Irradiation

The entire setup was irradiated with DT neutrons at the Frascati Neutron Generator facility [26]. Neutrons were generated from a beam of deuterium impinging on a tritium target, as illustrated in Fig. 4. Due to the reaction kinematics, the energy of neutrons is direction-dependent and it is equal to 14.07 MeV in a direction perpendicular to the ion beam

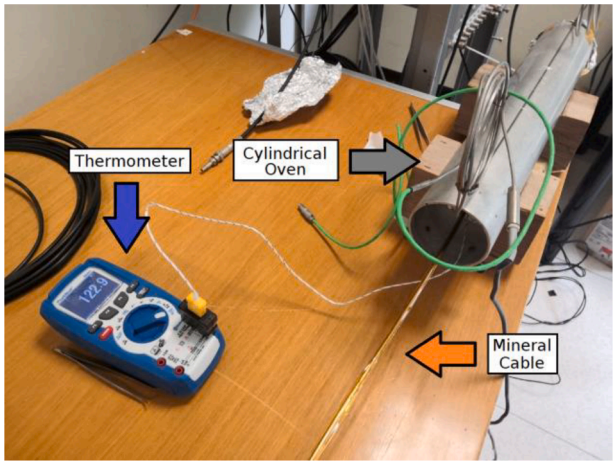

Fig. 3. Cylindrical oven (on the top right, gray arrow) in which the SiC detector is inserted. The mineral cable, enveloped in a Kapton foil, can be seen emerging from the oven (orange arrow). On the left a multimeter is measuring the temperature inside the oven (blue arrow). The thermistor is inside the oven, in the vicinity of the SiC active volume.

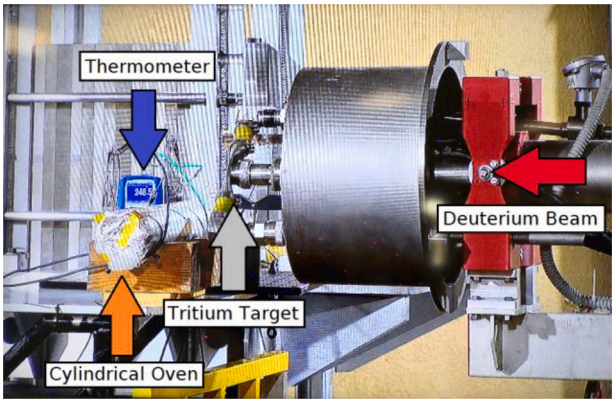

Fig. 4. The experimental setup - the oven containing the SiC and the cable (orange arrow) plus the thermistor and the multimeter temperature readout (blue arrow) - is on the left, placed in front of the FNG tritium target in the centre. The deuterium beam (on the right, red arrow) impinges on the target (small T-shaped pipe in the centre, gray arrow), producing DT neutrons along the entire solid angle.

[25]. It was not possible to insert the detector setup (and relative mineral cable and oven) on a perpendicular line of sight, so the detector was placed on a 45° angle with respect to the beam, allowing for a flux of neutron with a spectrum centred at 14.6 MeV [26].

Measurements were performed under neutron irradiation at different temperatures (100 °C, 150 °C, 200 °C and 250 °C). The temperature set point was reached and maintained within +/- 5 °C by acting directly on the current flowing into the electric resistance. Each irradiation lasted between 15 and 45 minutes, resulting in a neutron yield between $1.5 \cdot 10^{13}$ and $6.0 \cdot 10^{13}$ for each irradiation. A run at room temperature (around 25 °C) was also performed before the HT irradiations as reference.

3. Results

Signals detected were used to perform a pulse integral (PI) analysis. PI values were calibrated by matching the most prominent SiC spectral features to the known energy of the reaction channels (see [17] for details) to obtain the deposited energy (E_d) spectra. One of these is plotted in Fig. 5 as an example. The features are fitted with either gaussian functions (in the case of two-body nuclear reactions involving only charged particles as products) or step function convoluted with a gaussian (in the case of three-body reactions or reactions involving a neutron as products): this is due to the fact that the former are expected to produce a specific E_d while the latter are expected to feature a continuous spectrum of E_ds up to a threshold. The mean value μ, the amplitude a and the standard deviation σ of the fits are used to calculate the FWHM (obtained as $FWHM = \sqrt{2ln2} \cdot 2\sigma$) and area A (as $A = a\sqrt{2\pi\sigma^2}$) of the fits. These values, along with the mean value of the gaussian, are significant to monitor the changes of the detection properties of the detector: the mean value measures changes in the response function, the area measures variations in the efficiency and the ratio between FWHM and the mean value measures the energy resolution ($\epsilon = FWHM/\mu$).

All the calibrated spectra are plotted in Fig. 6 for comparison, after being normalized to 10^{13} neutrons produced in the target during each irradiation. The spectral features of the 100 °C, 150 °C, 200 °C and 250 °C overlap significantly to the features of the room temperature spectrum for deposited energies greater than 2500 keV, which is the low-energy cutoff already used in [9] to avoid low-E_d noise.

In Fig. 7 the mean value, the area and the energy resolution of the gaussian fits of the $^{12}C(n,\alpha)^{9}Be$ reaction (which is the most significant feature to be used for spectroscopic measurements [17]) are plotted as a function of the temperature in order to measure their change in temperature. The error bars in Fig. 7 are due to the statistical uncertainty in the FNG neutron emission (+/-5 %) and to uncertainties derived from the energy calibration and from the gaussian fits of the spectra. The Fig. shows that the pulse integral mean value is compatible with a stable value in temperature, suggesting that the response function is not changed with rising temperature. The area of the integral oscillates more around the mean value, having values that (on average) differ from the mean by 1.8 times the standard deviation. This, combined with an absence of a trend with temperature, suggests that SiC efficiency uncertainties could be underestimated. One possible source of error might be the partial depletion operation introducing uncertainties in the size of the depletion region and, thus, on the efficiency of the detector: this hypothesis should be explored in the future operating in HT a thinner SiC in full depletion mode. Lastly, the energy resolution varies considerably with temperature - from a maximum of 9.8 % at 100 °C to a minimum of 6.1 % at 250 °C. The high χ^2 value (97.8) rules out this

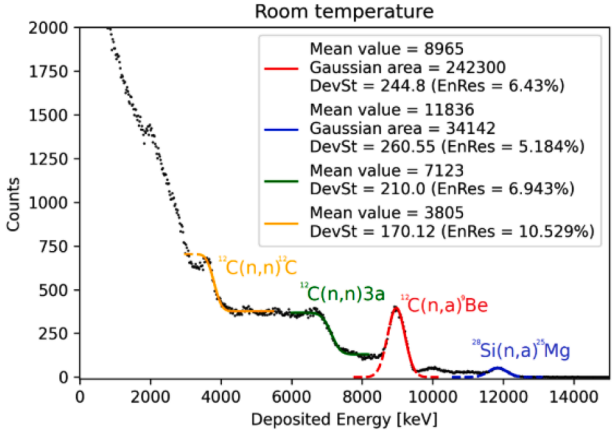

Fig. 5. Deposited energy spectrum obtained with the SiC at room temperature. The typical SiC spectral features are highlighted in different colours: $^{28}Si(n,\alpha)^{25}Mg$ (in blue), $^{12}C(n,\alpha)^{9}Be$ (in red), $^{12}C(n,n)3\alpha$ (in green) and the elastic scattering on carbon (in yellow). All the features are fitted with either a gaussian function or a step-function convoluted to a gaussian. The mean value μ and the standard deviation σ of the fits are reported, as well as the area underlying the gaussian fits for the two peaks. The energy resolution of the detector is calculated as $\epsilon = \frac{2\sqrt{2ln2}\cdot\sigma}{\mu}$ and it is reported within brackets.

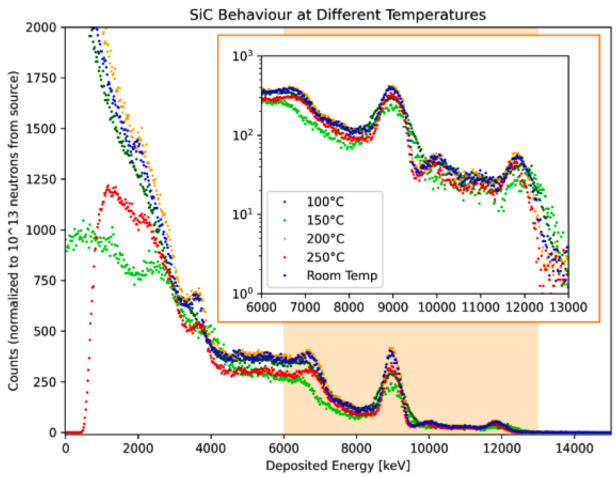

Fig. 6. Comparison between the deposited energy spectrum (after normalization to 10^{13} neutrons produced by the neutron source) obtained at different temperatures. The similarities between the spectra at HT and the spectra at RT for the reactions at high E_ds ($E_d > 6000$ keV, highlighted in orange and plotted in a y-axis logarithmic scale on the top-right) are used to compare the performance of the SiC at various temperatures.

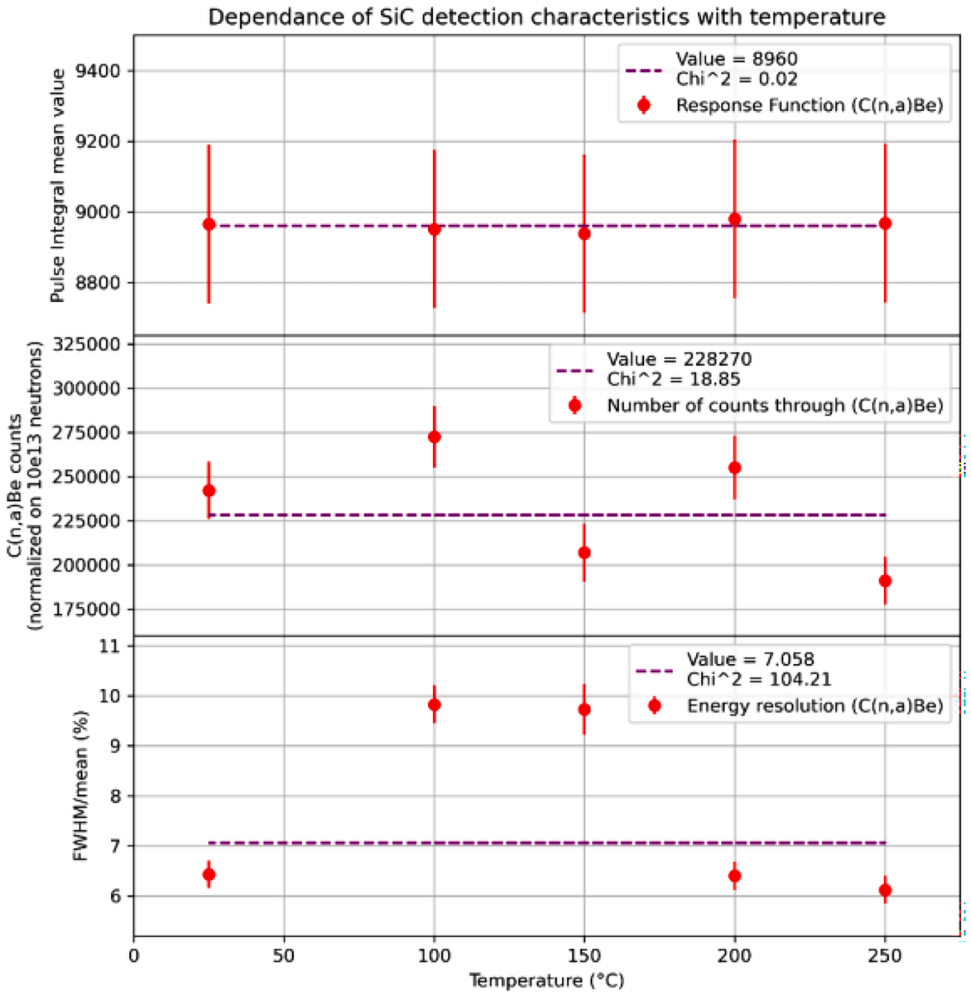

Fig. 7. Evolution of the detection characteristics of the SiC as a function of the temperature (on the x-axis), calculated using the $^{12}C(n,\alpha)^{9}Be$ reaction. On top, the mean value of the fit is used to monitor the response function of the detector. In the middle the area of the gaussian fit is used to measure the number of counts through the reaction (normalized to the same number of neutrons produced by the source), which is thus proportional to the efficiency. At the bottom the ratio between FWHM and mean value is used as a reference for the energy resolution. Data are presented with their uncertainties. The χ^2 value obtained by fitting the three data sets with a horizontal line is used to assess the likelihood of the three detection characteristics being constant over the analysed temperature range. While the response function can be assumed to be constant, the efficiency shows fluctuations that exceed slightly the error bars, suggesting an underestimation of the errors. Energy resolution (having a very high χ^2 of 97.8) is also incompatible with its errors, suggesting that 100 °C and 150 °C might be outliers.

being due to uncertainties in the measurement. It must be noted that the RT, 200 °C and 250 °C spectra are compatible between them since their mean (6.3 %) is within one standard deviation from all three data points. The same trend can be verified calculating the energy resolution on the other spectral features. This suggests that 100 °C and 150 °C might be outliers, either due to systematic errors, SiC material or detector properties. One possible cause of systematic error is the 100 °C and 150 °C spectra being performed with a temperature oscillating more than RT and 200 °C/250 °C irradiations, thus worsening the calibration quality. To assess this, new investigations will be performed in the future with a finer temperature control and different setups (different crystal, different metallization, etc.).

4. Summary

In this paper the detection performances of a SiC neutron detector prototype were tested at high temperatures under irradiation of DT neutrons (with 14.6 MeV energy). The experimental setup was chosen similar to the one used by Angelone in [13] in order to compare the results with diamond. While diamonds tested in the past appear to experience a degradation in the response function after 220 °C (see [13] and Fig. 23.a from [5]), the SiC demonstrated the ability of performing neutron counting and spectroscopy up to 250 °C. Statistical analysis revealed that the response function of the SiC is not altered by the increasing temperature. Energy resolution was also measured, finding that resolution at RT is equal to the one obtained at 200 °C and 250 °C but different than the one obtained at 100 °C and 150 °C. Upcoming works will determine if this behaviour is due to the experimental apparatus or to the SiC detector itself. Efficiency also varies in a way that doesn't depend on temperature but that doesn't overlap with the uncertainties of the measurement either, suggesting that partial depletion operation might introduce a source of uncertainty in the calculated efficiency: this calls for further investigations with a SiC in full depletion mode. The setup should also be improved by adopting either a spring-based or a high-temperature welded electrical contact to enhance solidity. Activities in the near future will also try to characterize the detector for higher temperatures to match the temperatures expected inside ITER's breeding blanket (300 °C – 550 °C [4]).

CRediT authorship contribution statement

Matteo Hakeem Kushoro: Writing – original draft, Visualization,

Software, Investigation, Formal analysis, Data curation, Conceptualization. **Maurizio Angelone:** Writing – review & editing, Resources, Methodology, Investigation, Conceptualization. **Daniele Bozzi:** Investigation, Data curation. **Stephanie Cancelli:** Writing – review & editing. **Andrea Dal Molin:** Writing – review & editing, Formal analysis. **Erik Gallo:** Investigation, Data curation. **Giuseppe Gorini:** Funding acquisition. **Francesco La Via:** Writing – review & editing, Resources. **Miriam Parisi:** Funding acquisition. **Enrico Perelli Cippo:** Investigation, Data curation. **Oscar Putignano:** Software. **Marco Tardocchi:** Project administration, Conceptualization. **Marica Rebai:** Supervision, Conceptualization.

Declaration of competing interest

The authors declare that they have no known competing financial interests or personal relationships that could have appeared to influence the work reported in this paper.

Data availability

Data will be made available on request.

Acknowledgments

A special thanks goes to the Joint Research Agreement Eni-CNR (Linea 5), whose contribution was instrumental in making progress with the research activity. In particular, the authors would like to acknowledge the critical contributions from Erik Gallo and Miriam Parisi.

References

[1] G. Federici et al., An overview of the EU breeding blanket design strategy as an integral part of the DEMO design effort, Fusion Engineering and Design, Volume 141, April 2019, Pages 30-42.
[2] L.M. Giancarli et al., Overview of the ITER TBM program, fusion engineering and design, Volume 87, Issues 5–6, August 2012, Pages 395-402.
[3] S. Segantin, et al., Neutronic comparison of liquid breeders for ARC-like reactor blankets, Fusion Eng. Design 160 (November 2020) 112013.
[4] L.M. Giancarli, et al., Tritium and heat management in ITER Test Blanket Systems port cell for maintenance operations, Fusion Eng. Design 89 (2014) 2088–2092.
[5] M. Angelone, C. Verona, Properties of diamond-based neutron detectors operated in harsh environments, J. Nucl. Eng. 2 (4) (2021) 422–470.
[6] L. Giacomelli, Neutron emission spectroscopy of DT plasmas at enhanced energy resolution with diamond detectors, Rev. Scient. Instrum. 87 (2016) 11D822.
[7] M. Rebai et al., Response of a single-crystal diamond detector to fast neutrons, JINST 8 P10007.
[8] M. Hodgson, et al., Characterization of silicon carbide and diamond detectors for neutron applications, Meas. Sci. Technol. 28 (2017) 105501, 13pp.
[9] M. Rebai, et al., New thick silicon carbide detectors: Response to 14 MeV neutrons and comparison with single-crystal diamonds, Nuclear Inst. Methods Phys. Res. 946 (2019) 162637. A.
[10] M. De Napoli, SiC detectors: A review on the use of silicon carbide as radiation detection material, Front. Phys. 10:898833.
[11] D. Rigamonti, et al., Neutron spectroscopy measurements of 14 MeV neutrons at unprecedented energy resolution and implications for deuterium–tritium fusion plasma diagnostics, Measure. Sci. Techn. 29 (2018) 045502, 9pp.
[12] M. Tardocchi, et al., A high-resolution neutron spectroscopic camera for the SPARC tokamak based on the Jet European Torus Deuterium-Tritium experience, Rev. Sci. Instrum. 93 (11) (2022 Nov 1) 113512.
[13] M. Angelone, et al., Systematic study of the response of single crystal diamond neutron detectors at high temperature, J. Instrumentat. 15 (March 2020).
[14] C. Weiss, et al., High-temperature performance of solid-state sensors up to 500°C, Nuclear Inst. Methods Phys. Res. 1040 (2022) 167182. A.
[15] D. Szalkai, et al., Fast neutron detection with 4H-SiC based diode detector up to 500°C ambient temperature, IEEE Transact. Nuclear Sci. 63 (3) (June 2016).
[16] F.H. Ruddy, Performance and Applications of Silicon Carbide Neutron Detectors in Harsh Nuclear Environments, EPJ. Web. Conf. 253 (2021) 11003.
[17] M.H. Kushoro, et al., Silicon Carbide characterization at the n_TOF spallation source with quasi-monoenergetic fast neutrons, Nuclear Inst. Methods Phys. Res. 983 (2020) 164578. A.
[18] M.H. Kushoro, et al., Detector response to D-D neutrons and stability measurements with 4H silicon carbide detectors, Materials 14 (2021) 568.
[19] M.H. Kushoro, et al., Performance of a thick 250 um silicon carbide detector: stability and energy resolution, JINST 18 (2023) C03007.
[20] M.H. Kushoro, et al., Partially depleted operation of 250 μm-thick silicon carbide neutron detectors, Nuclear Inst. Methods Phys. Res. 1058 (2024) 168918. A.
[21] S. Tudisco, et al., SiCILIA—silicon carbide detectors for intense luminosity investigations and applications, Sensors 18 (2018) 2289.
[22] F. La Via et al., Silicon carbide devices for radiation detection and measurements, J. Phys.: Conf. Ser. 1561 012013.
[23] A. Meli, et al., Epitaxial growth and characterization of 4H-SiC for neutron detection applications, Materials 14 (2021) 976.
[24] Available online: https://cividec.at/electronics-Cx-L.html.
[25] Available online: https://www.caen.it/products/dt5730/.
[26] A. Pietropaolo, et al., The Frascati Neutron Generator: A multipurpose facility for physics and engineering, in: IOP Conf. Series: Journal of Physics: Conf. Series 1021, 2018 012004.